Structural Insights from Tandem Mass Spectrometry, Ion mobility-Mass Spectrometry, and Infrared/Ultraviolet Spectroscopy on Sphingonodin I: Lasso vs. Branched-cyclic Topoisomers

Kevin Jeanne Dit Fouque,[†] Valeriu Scutelnic,[‖] Julian D. Hegemann,[‡] Sylvie Rebuffat,[§] Philippe Maître,[#] Thomas R. Rizzo[‖] and Francisco Fernandez-Lima.*[,†]

[†] Department of Chemistry and Biochemistry, Florida International University, 11200 SW 8th St., AHC4-233, Miami, FL 33199, United States.

[‖] Laboratory of Molecular Physical Chemistry, Ecole Polytechnique Fedérale de Lausanne, Station 6, CH-1015 Lausanne, Switzerland.

[‡] Institute of Chemistry, Technische Universität Berlin, Straße des 17. Juni 124, 10623, Berlin, Germany

[§] Laboratory Molecules of Communication and Adaptation of Microorganisms, National Museum of Natural History, CNRS, 57 rue Cuvier, CP-54, 75005 Paris, France.

[#] Laboratoire de Chimie Physique, Université Paris Sud, UMR 8000 CNRS, Faculté des Sciences, Bât. 349, 91405 Orsay Cedex, France.

ABSTRACT: Lasso peptides form a class of ribosomally synthesized and post-translationally-modified peptides (RiPPs) characterized by a mechanically interlocked topology, where the C-terminal tail of the peptide is threaded and trapped within an N-terminal macrolactam ring. Sphingonodin I is a lasso peptide that has not yet been structurally characterized using the traditional structural biology tools (e.g., NMR and X-ray crystallography) and its biological function has not yet been elucidated. In the present work, we describe structural signatures characteristic of the class II lasso peptide sphingonodin I and its branched-cyclic analog using a combination of gas-phase ion tools (e.g., tandem mass spectrometry, MS/MS, trapped ion mobility spectrometry, TIMS, and infrared, IR, and ultraviolet, UV, spectroscopies). Tandem MS/MS CID experiments on sphingonodin I yielded mechanically interlocked species with associated b_i and y_j fragments demonstrating the presence of a lasso topology, while tandem MS/MS ECD experiments on sphingonodin I showed a significant increase in hydrogen migration in the loop region when compared to the branched-cyclic analog. The high mobility resolving power of TIMS permitted the separation of both topoisomers, where sphingonodin I adopted a more compact structure than its branched-cyclic analog. Cryogenic and room-temperature IR spectroscopy experiments evidenced a different hydrogen bond network between the two topologies, while cryogenic UV spectroscopy experiments clearly demonstrated a distinct phenylalanine environment for the lasso peptide.

1. INTRODUCTION

Lasso peptides are a structurally unique class of ribosomally synthesized and post-translationally modified peptides (RiPPs) that display a mechanically interlocked topology, where the N-terminal macrolactam ring is crossed by the C-terminal tail (Figure S1) [1-4]. The lasso peptide fold is accomplished by the action of a set of enzymes encoded in the lasso peptide gene cluster that i) recognize the N-terminal leader region of the ribosomally synthesized precursor peptide, ii) proteolytically cleave the leader to release the α-amino group of the C-terminal core peptide, and iii) catalyze a condensation reaction between the N-terminal α-amino group of the core peptide with the carboxylic acid side chain of an Asp or Glu residue in an ATP-dependent manner [3-8]. This implies an appropriate pre-folding step, where the C-terminal tail is positioned in a way that allows the macrolactam ring to be formed around it and thus enclosing the tail inside the ring. The lasso fold is primarily maintained by steric interactions arising from bulky side chain residues serving as plugs, and sometimes assisted by disulfide bonds (Figure S1) [9-13]. Lasso peptides are grouped into four classes depending on the

presence (class I, III, and IV) or absence (class II) of specific disulfide linkages (Figure S1) [14]. The mechanically interlocked topology affords lasso peptides an interesting variety of biological activities, such as enzyme inhibition, receptor antagonism, antimicrobial or antiviral properties [1-4, 15]. Lasso peptides are generally resistant to most common proteases, extreme pH values and high temperature. However, unthreading of the C-terminal tail of certain class II lasso peptides, yielding their branched-cyclic topoisomers, can be triggered by prolonged incubation at elevated temperature [16-20]. In addition, specific peptidases are present in nature dedicated solely to lasso peptide degradation [21, 22]. These processes represent a limitation to the biological activity of these lasso peptides.

Sphingonodin I is a 17 residue class II lasso peptide originating from *Sphingobium japonicum*, for which no biological activity has been yet reported. It is composed of an eight residue macrolactam ring closed by an isopeptide bond between the α-amino group of Gly1 and the side chain carboxyl group of Asp8 (highlighted in green in Figure 1). This results in a loop of five residues located above the ring (highlighted in blue) and a C-terminal tail of four residues located below the ring (highlighted in orange) [16]. Traditional structural biology tools generally used for the structural characterization of lasso peptides, such as nuclear magnetic resonance (NMR) [23, 24] and X-ray crystallography [18, 21, 25-27], have not yet assigned the position of the plug residues that lock the sphingonodin I lasso topology. MS-based approaches using a combination of collision induced dissociation (CID) and electron transfer dissociation (ETD) have permitted the assignment of the Glu13 and Asn14 residues, located on each side of the ring (highlighted in red in Figure 1), as being responsible for the trapping of the C-terminal part in the macrolactam ring (plug residues) [27]. Cleavage within the loop region of upon CID generates mechanically interlocked species with associated N-terminal and C-terminal fragments through the steric hindrance provided by the Glu13 and Asn14 side-chains, indicating the presence of a lasso topology. In addition, sphingonodin I is not subject to temperature-induced unthreading [16], which makes it an interesting model to decipher the interactions responsible for its stabilization.

Electron capture/transfer dissociation (EC/TD) [27-29] and ion mobility spectrometry (IMS) [30-33] also allow for the differentiation between the lasso and branched-cyclic topologies, particularly in cases when the former do not yield mechanically interlocked product ions in CID. A complementary approach to these aforementioned techniques is infrared (IR) spectroscopy, which can provide information on the hydrogen-bond network that participates in the stabilization of both topologies. It has been reported that the IR spectroscopic data were fully consistent with the ion mobility data, in which strong evidence for a correlation between smaller/larger collision cross sections (CCS) and hydrogen-bond making/breaking were obtained between the lower charge states (e.g. $[M+3H]^{3+}$) and the highest charge state ($[M+4H]^{4+}$), respectively [34].

In the present work, sphingonodin I and its branched-cyclic topoisomer (Figure 1) were investigated using tandem mass spectrometry (CID and ECD), trapped ion mobility spectrometry (TIMS), cryogenic and room-temperature IR spectroscopies, and cryogenic ultraviolet (UV) spectroscopy. The CID and ECD fragmentation patterns, as well as the TIMS profiles, of the two topologies were compared to reveal lasso-specific structural signatures for sphingonodin I. Complementary experiments using cryogenic and room-temperature IR spectroscopies, with an optical parametric oscillator/amplifier (OPO/A), and room-temperature IR spectroscopy, with a free electron laser (FEL), were employed to derive information on the hydrogen bonding network that participates in the stabilization of the two topologies. Additional experiments using cryogenic UV spectroscopy in the region of phenylalanine chromophore absorption were used to probe the phenylalanine (Phe16) environment, located near the plug residues for the lasso peptide.

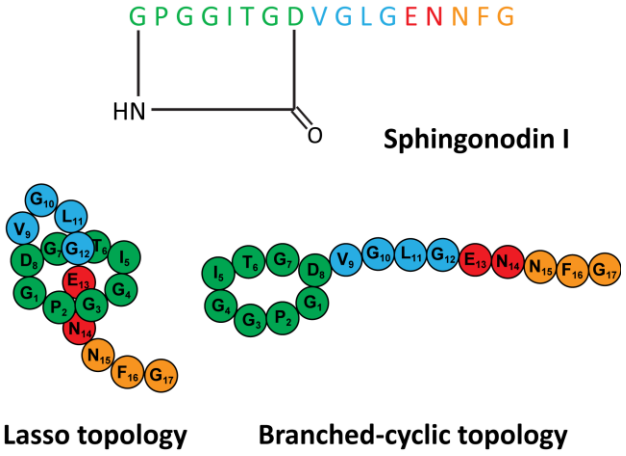

Figure 1. Sequences and schematics of sphingonodin I and its branched-cyclic analog. The macrolactam rings are colored in green, the loop residues in blue, the plugs in red and the C-terminal tail in orange.

2. EXPERIMENTAL SECTION

2.1. Materials and Reagents. Details on sphingonodin I production have been reported previously [16]. Briefly, sphingonodin I was produced heterologously in *Escherichia coli* BL21 (DE3) by IPTG-

induced expression of a pET41a production plasmid in M9 medium at 20 °C for 3 days. Sphingonodin I was extracted from the cell pellet with methanol and then purified by reversed-phase high performance liquid chromatography (RP-HPLC). As sphingonodin I is resistant to thermally induced unthreading [16, 20], the branched-cyclic analog was obtained by solid-phase synthesis from Genepep (St Jean de Védas, France). Solutions were prepared at a final concentration of 5 µM in 10 mM ammonium acetate (NH_4Ac) for native conditions.

2.2. ECD Experiments. ECD experiments were carried out on a Solarix 7T FT-ICR mass spectrometer (Bruker, Billerica, MA) equipped with a nanoESI source operating in the positive ion mode. Sample aliquots (10 µL) were loaded in a pulled-tip capillary mounted on a custom built XYZ stage in front of the MS capillary inlet. The ESI voltage, capillary exit, and skimmers I and II were set to 1500 V, 200 V, 50 V and 16 V, respectively. ECD experiments were performed with a heated hollow cathode operating at a current of 1.6 A. Electrons emitted during 0.2 s were injected into the ICR cell with a 1.5 V bias and 16 V ECD lens.

2.3. TIMS Experiments. Ion mobility experiments were performed on a custom built nanoESI-TIMS coupled to an Impact Q-ToF mass spectrometer (Bruker, Billerica, MA, Figure S2). The TIMS unit is controlled using a custom software in LabView (National Instruments) synchronized with the MS platform controls [35]. Details regarding the TIMS operation (Figure S2) and calibration procedure can be found elsewhere [35-38]. Peptide sample solutions were loaded in a pulled-tip capillary mounted in a custom built XYZ stage in front of the MS inlet. A typical 800-1000 V between the capillary and the MS inlet was applied. TIMS experiments were carried out using nitrogen (N_2) as buffer gas at room temperature. The gas velocity was kept constant between the funnel entrance ($P1$ = 2.6 mbar) and exit ($P2$ = 1.1 mbar, Figure S2). An rf of 250 V_{pp} at 880 kHz was applied to all TIMS electrodes. A voltage ramp (V_{ramp}) of -250 to -50 V, a deflector voltage (V_{def}) of 60 V, and a base voltage (V_{out}) of 60 V were used for the separation of the two topoisomers. Collision induced dissociation (CID) experiments were performed in the collision cell located after the TIMS analyzer (Figure S2). The mass-selected $[M+2H]^{2+}$ ions were fragmented using nitrogen as collision gas at a collision energy of 22 eV.

2.4. Room-temperature IR Spectroscopy. IR spectroscopy experiments were performed employing a 7 T FT-ICR mass spectrometer (Apex Qe, Bruker) equipped with tunable infrared lasers. A detailed layout of this experimental apparatus is described elsewhere [39]. The mass-selected $[M+2H]^{2+}$ ions were accumulated in an argon pressurized (~ 10^{-3} mbar) linear hexapole ion trap and were then pulse extracted and stored in the ICR cell where they were irradiated with infrared light. The most abundant fragments observed upon infrared activation for the mass-selected $[M + 2H]^{2+}$ ions of sphingonodin I and sphingonodin I branched-cyclic were the loss of a water molecule ($[M+2H-H_2O]^{2+}$) as well as y_6, b_{11} and b_{16}^{2+} product ions. Other fragment channels which led to very low ion intensities and did not significantly affect the photodissociation efficiencies were not used in the calculations. IR spectra were recorded in the 2800–3700 cm^{-1} spectral range using an OPO/A (Laser-Vision, Bellevue, WA) benchtop system. Two different OPA settings were used to optimize the laser output energy in the 2800–3400 cm^{-1} and 3400–3700 cm^{-1} spectral regions. The OPO irradiation time was 1 s with a CO2 (BFI Optilas, Evry, France) pulse length of 2 ms to enhance the infrared induced fragmentation efficiency. IR spectroscopy in the 1350–1800 cm^{-1} spectral range was performed using the infrared free electron laser (IR FEL, from CLIO, Orsay, France) [40]. The IR FEL irradiation time was set to 500 ms to record vibrational spectra in the mid-infrared.

2.5. Cryogenic IR/UV Spectroscopy. A detailed layout of the instrument used for cryogenic IR and UV spectroscopy is described elsewhere [41]. The mass-selected $[M+2H]^{2+}$ ions were trapped and cooled by collisions with helium buffer gas in a cryogenic octupole trap (3.5 K). UV and IR beams irradiated the ion cloud. UV spectra were acquired counting the Phe side-chain loss fragments with a channeltron detector placed after an analyzing quadrupole. Phenylalanine side-chain loss occurred from the electronic excited state of Phe and can be increased by vibrationally exciting the peptides that have absorbed a UV photon, as previously described [42]. We achieved large enhancement of the Phe side chain loss fragmentation shining infrared light (3310 cm^{-1}) 100 ns after a UV pulse. Cryogenic infrared spectra were obtained by means of the He-tagging technique [43]. In short, at the low temperature of the octupole trap part, the peptide ions were tagged with helium atoms. Before unloading the trap, an IR OPO/A beam was overlapped with the ions. The He-tagged peptides that absorb IR radiation lose their weakly bound He atom, causing depletion of the tagged-ion signal.

3. RESULTS AND DISCUSSION

3.1. Sphingonodin I MS/MS CID signatures. The analysis of sphingonodin I and its branched-cyclic form resulted in the observation of a single charge state species ($[M+2H]^{2+}$) under native conditions. The CID spectra of the $[M+2H]^{2+}$ ions of sphingonodin I (m/z 771.8) and the branched-cyclic analog are illustrated in Figure S3a and S3b, respectively. The CID spectrum of the lasso peptide showed a complicated fragmentation pattern that

involves a classic b_i/y_j series, corresponding to fragmentations in the C-terminal tail of sphingonodin I, as well as mechanically interlocked product ions with associated b_i and y_j fragments as illustrated in Figure S3a. These fragments remain associated through steric interactions imparted by the two bulky Glu13/Asn14 side-chain residues, which entrap the C-terminal part inside the macrolactam ring, as previously reported for class II lasso peptides [27, 44]. Such mechanically interlocked product ions clearly evidence the presence of a lasso topology for sphingonodin I. The CID spectrum of the $[M+2H]^{2+}$ ions of the branched-cyclic topoisomer

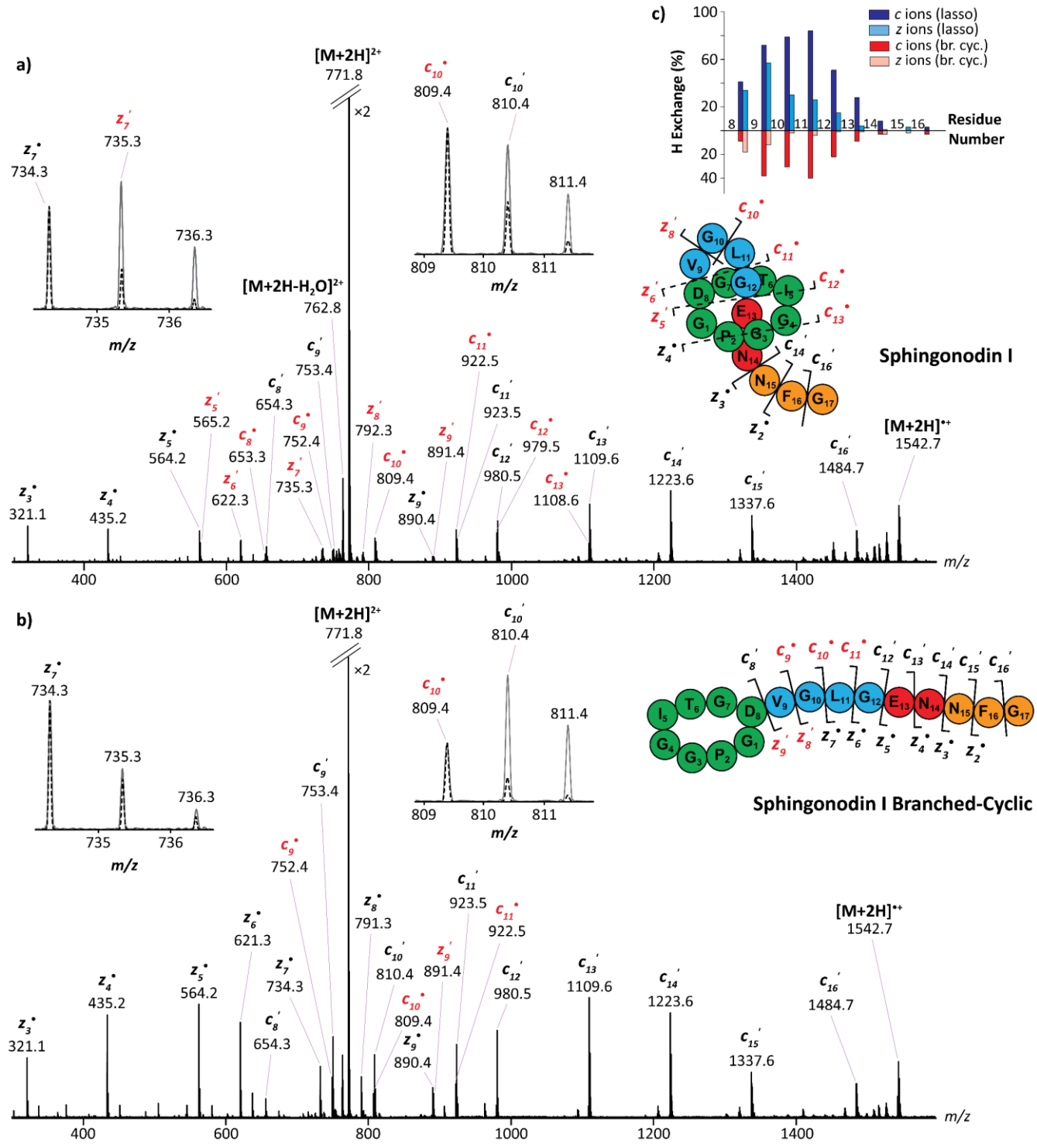

Figure 2. Typical MS/MS ECD spectra of the $[M+2H]^{2+}$ ions of (a) sphingonodin I and (b) the branched-cyclic topoisomer (*m/z* 771.8). Typical hydrogen migration events are highlighted in red and labeled on the peptide cartoons (right of each panel). (c) Bar plot showing the hydrogen migration events of sphingonodin I (blue bars) and the branched-cyclic topoisomer (red bars) obtained by correcting the contribution of the theoretical isotope patterns (black dashed lines in insets) to the experimental isotopic distribution (gray traces in insets). The macrolactam rings, the loop residues, the plugs and the C-terminal tails are highlighted in green, blue, red and orange, respectively.

did not exhibit any of the mechanically interlocked product ions and was only dominated by b_i/y_j fragments (Figure S3b). Sphingonodin I could therefore be differentiated from the branched-cyclic analog by CID.

3.2. Sphingonodin I MS/MS ECD signatures. A limitation to CID is that the mechanically interlocked product ions are only observed for class II lasso peptides, in which the loop is strictly longer than four amino acid residues [27]. We previously demonstrated the utility of ETD/ECD for identifying class II lasso peptide topologies as an alternative fragmentation approach to overcome the limited structural information provided by CID experiments [27]. ECD spectra of sphingonodin I (Figure 2a) and the branched-cyclic topoisomer (Figure 2b) were for the first time compared, for which a very similar fragmentation pattern was observed for the $[M+2H]^{2+}$ ions. Both topologies presented the charge-reduced $[M+2H]^{\bullet+}$ ions (*m/z* 1542.7) and classic $c'_i/z_j^{\bullet}$ fragment series, consisting of c'_8 to c'_{16} together with their complementary $z_9^{\bullet}$ to $z_2^{\bullet}$ (except $z_1^{\bullet}$, Figure 2) fragments. ECD spectra of sphingonodin I also displayed an increase of hydrogen migration events (H• transfer) near the loop region (Val9-Glu13) when compared to the branched-cyclic topoisomer, as previously reported for lasso peptides (Figure 2c) [27-29]. In fact, the c'_8 to c'_{13} product ions of the lasso topology were partially shifted by 1 Da from a loss of H•, leading to the formation of the $c_8^{\bullet}$ to $c_{13}^{\bullet}$ fragments, while their complementary $z_9^{\bullet}$ to $z_5^{\bullet}$ (except $z_4^{\bullet}$) product ions were partially shifted by 1 Da from a capture of H•, yielding the z'_9 to z'_5 fragments (highlighted in red in Figure 2a). Conversely, these mass-shifted product ions were substantially lower in relative intensity for the branched-cyclic topology (Figures 2b and 2c), indicating that the hydrogen migration events in the Val9-Glu13 region occurred less frequently in the absence of a lasso structure. Sphingonodin I could therefore be differentiated from the branched-cyclic analog by ECD through comparison of the hydrogen migration events. Note that the $c'_i/z_j^{\bullet}$ fragments having hydrogen migration events are actually a combination of both $c'_i/c_i^{\bullet}$ and $z_j^{\bullet}/z'_j$, as illustrated by the theoretical isotope patterns in the insets of Figure 2 (black dashed lines). Thus, the bar plots in Figure 2c were calculating by correcting the contribution of the theoretical isotope patterns to the experimental isotopic distribution (gray traces in the insets of Figure 2).

3.3. Sphingonodin I mobility separation. The ECD approach revealed itself to be useful for the differentiation between lasso and branched-cyclic topoisomers but is limited for the case of mixtures, for which the hydrogen migration events cannot be determined, since both topologies present this feature. This lead to consider TIMS as an alternative strategy, which proved to be very effective for the mobility separation between lasso and the unthreaded branched-cyclic analog [30]. Native TIMS spectra corresponding to the $[M+2H]^{2+}$ ions of sphingonodin I and the unthreaded branched-cyclic topoisomer are presented in Figure 3. Previous traveling wave IMS (TWIMS) experiments showed a single broad arrival-time distribution for the doubly protonated species of the lasso peptide (Figure 3, dashed line) [45]. Conversely, the high resolution TIMS analysis resulted in the identification of multiple IMS bands for the two topoisomers, providing additional insights about the structures adopted by the two topoisomers in native conditions (Figure 3). In addition, sphingonodin I and the branched-cyclic analog were clearly separated in TIMS, for which the branched-cyclic topology adopted significantly more extended structures than sphingonodin I, as previously reported using different IMS technologies [30, 31, 46]. Note that the present TIMS technology allows it to separate the two topologies at low charge state (native conditions), while artificially induced high charge states (denaturing conditions with supercharging reagents) are needed to discriminate the two topoisomers using TWIMS [31, 45, 46].

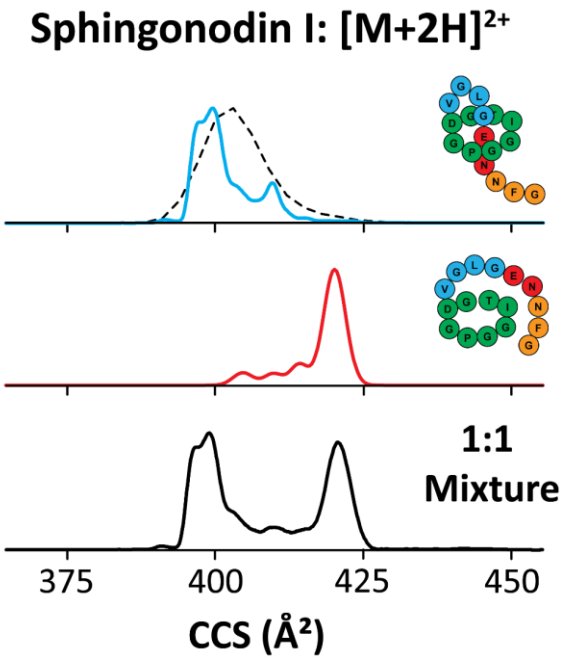

Figure 3. Typical TIMS spectra of the $[M+2H]^{2+}$ ions of sphingonodin I (blue trace), its branched-cyclic topoisomer (red trace) and in a 1:1 mixture (black trace). The black dashed line illustrates a previously reported TWIMS distribution [45]. Schemes highlight the macrolactam rings in green, the loop residues in blue, the plugs in red and the C-terminal tail in orange.

3.4. Sphingonodin I in room-temperature IR Spectroscopy. IR spectroscopy is a complementary approach to IMS-MS to derive structural insights on the intramolecular interactions of mass-selected ions [47]. The IR FEL and the OPO/A provide access to a wide frequency range, permitting the recording of vibrational spectra in the mid-infrared and in the X-H (X=C, N, O) stretching regions, respectively. These experiments were performed in an attempt to understand how the hydrogen bond network participates in the stabilization of the lasso peptide sphingonodin I and the unthreaded branched-cyclic topoisomer. IR spectra of the $[M+2H]^{2+}$ ions of sphingonodin I and its branched-cyclic form are shown in Figure 4a and 4b, respectively. A tentative assignment of the observed infrared bands is proposed in Table S1. Both topoisomers displayed similar IR bands in the high energy range (Figure 4). The IR bands observed at ~3560 cm^{-1} (highlighted in orange) are characteristic of free carboxylic OH C-terminal stretches [48, 49]. Those observed at ~3440 and ~3540 cm^{-1} can be assigned to free amide NH_2 *symmetric* and *asymmetric* stretches [50], respectively, arising from the side chains of asparagine (Asn14/Asn15) residues (highlighted in green). The IR bands at ~3480 cm^{-1} are a typical signature of free amide NH stretches [34, 50] of peptide bonds (highlighted in light purple). The relatively broad IR bands observed in the ~3040-3130 cm^{-1} spectral range are tentatively assigned to H-bonded carboxylic acid OH stretches [51], provided by the side chain of the Glu13 (highlighted in magenta). The presence of H-bonded carboxylic acid OH stretches was expected for the lasso topology due to the position of the Glu13 residue, which is literally inside the molecular knot (plug residue) and probably interact with the residues involved in the macrolactam ring. However, this feature was not expected for the branched-cyclic topology, for which the Glu13 residue is not located inside the molecular knot, suggesting that the C-terminal tail of the branched-cyclic topology is probably folded in close proximity to the macrolactam ring. Indeed, clear evidence for hydrogen bonding in the branched-cyclic topology could be observed in the ~3215-3415 cm^{-1} spectral range (highlighted in purple). This broad band could be assigned to red-shifted amide NH stretches [52, 53], confirming that the flexible C-terminal part

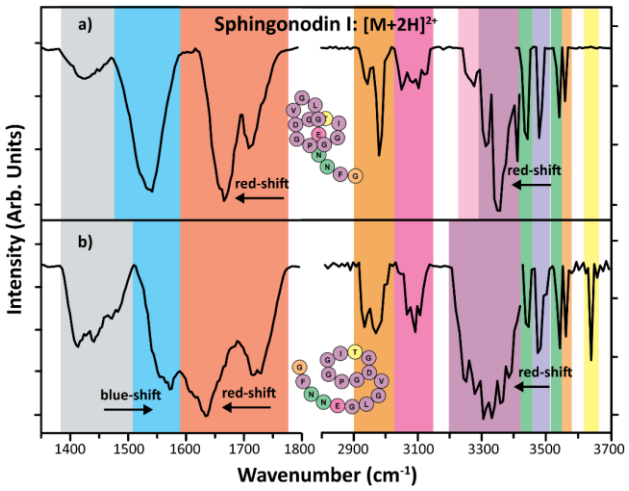

Figure 4. Typical IR spectra for the $[M+2H]^{2+}$ ions of (a) sphingonodin I and (b) the branched-cyclic topoisomer. The vibrational bands are assigned using a color coding as follows: gray (CH bend), blue (amide NH bend), red (carbonyl C=O stretch), brown (CH stretch), magenta (H-bonded carboxylic acid OH stretch), purple (H-bonded amide NH stretch), pink (H-bonded alcohol OH stretch), green (free NH_2 *sym.* and *asym.* stretches), light purple (free amide NH stretch), orange (OH C-terminal stretch) and yellow (free alcohol OH stretch).

is folded in close proximity to the macrolactam ring. This assignment was further supported by the IR spectrum in the 1350-1800 cm^{-1} spectral region. In fact, a blue-shifted amide NH bend [54, 55] band was observed at ~1570 cm^{-1} (highlighted in blue), with a red-shifted carbonyl C=O stretch [56, 57] band in the 1610-1670 cm^{-1} spectral region (highlighted in red). In addition, the presence of an IR band at ~3640 cm^{-1}, corresponding to free alcohol OH stretches [48, 58], provided supplementary structural

insights for the branched-cyclic topology (highlighted in yellow). This feature is evidence that the side-chain of Thr6 is free, indicating that the folding of the C-terminal part is probably not in close proximity to this residue. Moreover, no signal corresponding to free alcohol OH stretches (highlighted in yellow) at ~3640 cm^{-1} was observed for the lasso topology, suggesting that the Thr6 residue was likely involved in hydrogen bond interactions. As a result, the relatively broad IR band observed in the ~3240-3290 cm^{-1} was tentatively assigned to red-shifted alcohol OH stretches [53, 59] (highlighted in pink). Evidence for hydrogen bonding in the lasso topology could also be observed in the 3300-3415 cm^{-1} spectral range (highlighted in purple). Unresolved IR bands can be observed in this spectral region with three maxima at ~3305, 3350 and 3405 cm^{-1} corresponding to red-shifted amide NH stretches. This hydrogen bonding hypothesis was further supported by the 1350-1800 cm^{-1} spectral region, where red-shifted carbonyl C=O stretches at ~1665 cm^{-1} were observed (highlighted in red). However, the hydrogen bonding network of the lasso topology was found to be different from that of the branched-cyclic topology. A similar behavior was observed for the previously reported IR spectrum of the class II lasso peptide microcin J25, which adopts a short antiparallel β-sheet in the loop region [34]. This suggests that sphingonodin I also probably adopts a short antiparallel β-sheet in the Val9-Glu13 loop region that involves neutral hydrogen bonds between amide NH and CO groups.

3.5. Sphingonodin I in cryogenic IR/UV Spectroscopies. The cryogenic IR spectrum of the lasso peptide was more resolved than that of the branched-cyclic topoisomer (Figure 5a). Indeed, separate IR absorption bands that correspond to amide NH and NH_2 oscillators were clearly distinguishable, suggesting less structural variability for the lasso topology. The frequency range <3300 cm^{-1} was more crowded for the branched-cyclic topoisomer, which may be due to a more efficient hydrogen bonding network of the amide NH and NH_2 oscillators in a large number of conformers, which is in agreement with the findings from room-temperature IR experiments. In contrast to the room-temperature IR spectra, the free carboxylic acid OH C-terminal band at ~3560 cm^{-1} was only pronounced in the lasso topology, implying that the carboxylic group is predominantly free in the conformers of the lasso peptide. The branched-cyclic peptide instead did not show significant absorption at the C-terminal free carboxylic acid OH frequency. The resolved IR bands at >3400 cm^{-1} in the lasso topology pointed to the presence of a few amide groups that are fixed in a specific conformation. Conversely, one distinct absorption IR band at >3400 cm^{-1} was only observed in the branched-cyclic peptide. This feature suggests a larger variability in the amide group interactions with the neighboring polar groups. In general, the more flexible branched-cyclic peptide can freeze in many possible conformations at low temperature, which results in a less resolved spectrum. The locked structure of the lasso peptide is restricted to a smaller conformational space that leads to a more structured and sparse IR spectrum. Differences between cryogenic and room temperature IR spectra can thus occur because a range of conformers with distinct folding patterns can be trapped at low temperature.

Cryogenic UV spectroscopy in the region of phenylalanine chromophore absorption is a sensitive probe of the phenylalanine environment. In the case of the lasso topology, UV-induced fragmentation was very weak, probably suggesting that the Phe16 side chain strongly binds to the rest of the peptide (Figure 5b, blue traces). The large continuous absorption was due to a variability in the Phe chromophore interactions with the lasso peptide backbone that gives rise to a multitude of vibronic transitions. The UV spectrum of the branched-cyclic topology was more structured than that of the lasso peptide, where three strong absorption UV bands (37442, 37446 and 37535.2 cm-1) were obtained that repeat 532 cm^{-1} further in a vibrational progression due to the phenylalanine chromophore bending (Figure 5b, red traces) [60, 61]. The intense UV bands appeared near the frequency of the band origin in the protonated amino acid (37520.9 cm^{-1}) [60], suggesting that the phenylalanine chromophore is weakly interacting with

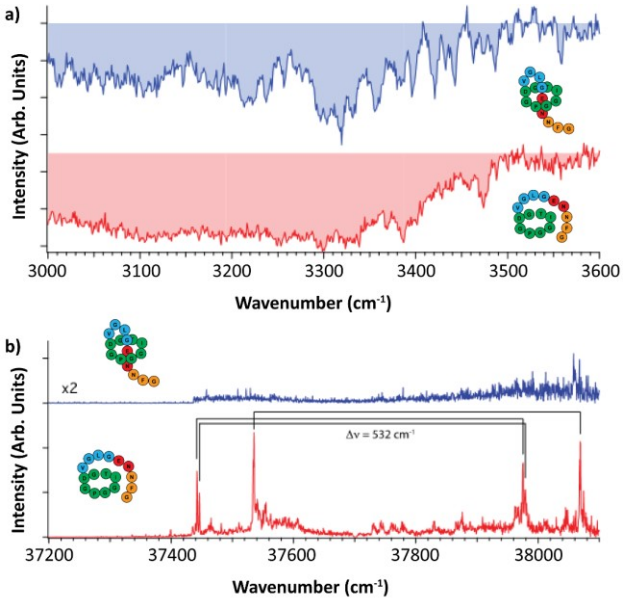

Figure 5. Typical cryogenic (a) IR and (b) UV spectra for the $[M+2H]^{2+}$ ions of sphingonodin I (blue traces) and the branched-cyclic topoisomer (red traces).

the backbone of the branched-cyclic peptide. The intense UV absorption bands of the branched-cyclic topology were absent in the UV spectrum of the lasso topology, suggesting a different folding pattern for the lasso peptide that strongly affects the phenylalanine residue. Overall, the fragmentation yield was significantly lower in the case of the lasso peptide. The presented results therefore allowed us to hypothesize that the aromatic chromophore strongly interacts with the backbone and very probably with the macrolactam ring, suggesting that the Phe16 residue plays a role in the stabilization of the C-terminal part inside the macrolactam ring. In fact, it was surprising that the relatively small side chain of Asn14 resulted in a lasso peptide that is not sensitive to thermal unthreading [16]. We suggest that Glu13 and Asn14 remain the primary plugs based on the MS observation, but that a proper folding of the C-terminal tail probably makes Phe16 forming a cork together with Asn14 that completely locks the lasso fold more efficiently than Asn14 could do by itself, as previously described for microcin J25 [62].

4. CONCLUSIONS

The lasso peptide sphingonodin I and the corresponding branched-cyclic topoisomer were studied using complementary gas-phase ion tools. The MS/MS CID experiments were effective for the differentiation between the two topoisomers by specifically yielding mechanically interlocked product ions for the lasso topology only. Likewise, MS/MS ECD was also effective by specifically showing a larger extent of hydrogen migrations near the loop region of the lasso topology, when compared to the branched-cyclic analog. The high resolution TIMS resulted in the clear separation of both topoisomers under native conditions, where sphingonodin I adopted a more compact structure than the branched-cyclic analog. This is fundamental since previous TWIMS experiments with lasso peptides required the artificial induction of high charge states by addition of a supercharging agent under denaturing conditions to achieve separation.

Cryogenic and room-temperature IR spectroscopy experiments evidenced a different hydrogen bonding network between the two topologies, where the lasso topology probably adopts a short antiparallel β-sheet in the Val9-Glu13 loop region while the flexible C-terminal part of the branched-cyclic topology is potentially folded in close proximity to the macrolactam ring. Cryogenic UV spectroscopy experiments clearly showed distinctly different phenylalanine environments for the two topoisomers. Whereas the phenylalanine chromophore only weakly interacts with the backbone of the branched-cyclic peptide, a strong backbone interaction of the phenylalanine chromophore is apparent in the lasso topology. This behavior suggests that Phe16 might be responsible for a secondary interaction that strengthens the stabilization of the lasso fold, making it resistant to thermal unthreading. It thus seems that the present findings can constitute a step forward in understanding the mode of stabilization of sphingonodin I, which has a small lower plug (below the ring), but does not unthread upon temperature increase.

ASSOCIATED CONTENT

Supporting Information

Supporting Information contain additional Figures that illustrate the general classification criteria for lasso peptides, that depict the TIMS-MS instrument by showing the TIMS cell schematic and TIMS operation, and that show the CID spectra of the $[M+2H]^{2+}$ ions of sphingonodin I and the branched-cyclic topoisomer. The SI also contains a Table summarizing the measured experimental vibrational frequencies (cm^{-1}) for the $[M+2H]^{2+}$ ions of sphingonodin I and the branched-cyclic topoisomer in the 1350-1800 and 2800-3700 cm^{-1} spectral regions. This material is available free of charge via the Internet at http://pubs.acs.org.

AUTHOR INFORMATION

Corresponding Author

* Email: fernandf@fiu.edu

Author Contributions

The manuscript was written through contributions of all authors. All authors have given approval to the final version of the manuscript.

Notes

The authors declare no competing financial interest.

ACKNOWLEDGEMENTS

The authors acknowledge the financial support from the National Science Foundation Division of Chemistry, under CAREER award CHE-1654274, with co-funding from the Division of Molecular and Cellular Biosciences to FFL. TRR and VS also thank the Swiss National Science Foundation for the support of this work under grant No. 200020_165908.

REFERENCES

1. Hegemann, J.D., Zimmermann, M., Xie, X., Marahiel, M.A.: Lasso peptides: an intriguing class of bacterial natural products. Acc. Chem. Res. **48**, 1909-1919 (2015)
2. Maksimov, M.O., Pan, S.J., James Link, A.: Lasso peptides: structure, function, biosynthesis, and engineering. Nat. Prod. Rep. **29**, 996-1006 (2012)
3. Arnison, P.G., Bibb, M.J., Bierbaum, G., Bowers, A.A., Bugni, T.S., Bulaj, G., Camarero, J.A., Campopiano, D.J., Challis, G.L., Clardy, J., Cotter, P.D., Craik, D.J., Dawson, M., Dittmann, E., Donadio, S., Dorrestein, P.C., Entian, K.D., Fischbach, M.A.,

Garavelli, J.S., Goransson, U., Gruber, C.W., Haft, D.H., Hemscheidt, T.K., Hertweck, C., Hill, C., Horswill, A.R., Jaspars, M., Kelly, W.L., Klinman, J.P., Kuipers, O.P., Link, A.J., Liu, W., Marahiel, M.A., Mitchell, D.A., Moll, G.N., Moore, B.S., Muller, R., Nair, S.K., Nes, I.F., Norris, G.E., Olivera, B.M., Onaka, H., Patchett, M.L., Piel, J., Reaney, M.J., Rebuffat, S., Ross, R.P., Sahl, H.G., Schmidt, E.W., Selsted, M.E., Severinov, K., Shen, B., Sivonen, K., Smith, L., Stein, T., Sussmuth, R.D., Tagg, J.R., Tang, G.L., Truman, A.W., Vederas, J.C., Walsh, C.T., Walton, J.D., Wenzel, S.C., Willey, J.M., van der Donk, W.A.: Ribosomally synthesized and post-translationally modified peptide natural products: overview and recommendations for a universal nomenclature. Nat. Prod. Rep. **30**, 108-160 (2013)

4. Montalban-Lopez, M., Scott, T.A., Ramesh, S., Rahman, I.R., van Heel, A.J., Viel, J.H., Bandarian, V., Dittmann, E., Genilloud, O., Goto, Y., Grande Burgos, M.J., Hill, C., Kim, S., Koehnke, J., Latham, J.A., Link, A.J., Martinez, B., Nair, S.K., Nicolet, Y., Rebuffat, S., Sahl, H.G., Sareen, D., Schmidt, E.W., Schmitt, L., Severinov, K., Sussmuth, R.D., Truman, A.W., Wang, H., Weng, J.K., van Wezel, G.P., Zhang, Q., Zhong, J., Piel, J., Mitchell, D.A., Kuipers, O.P., van der Donk, W.A.: New developments in RiPP discovery, enzymology and engineering. Nat. Prod. Rep. (2020)

5. Hegemann, J.D., Schwalen, C.J., Mitchell, D.A., van der Donk, W.A.: Elucidation of the roles of conserved residues in the biosynthesis of the lasso peptide paeninodin. Chem. Commun. **54**, 9007-9010 (2018)

6. Koos, J.D., Link, A.J.: Heterologous and in Vitro Reconstitution of Fuscanodin, a Lasso Peptide from Thermobifida fusca. J. Am. Chem. Soc. **141**, 928-935 (2019)

7. DiCaprio, A.J., Firouzbakht, A., Hudson, G.A., Mitchell, D.A.: Enzymatic Reconstitution and Biosynthetic Investigation of the Lasso Peptide Fusilassin. J. Am. Chem. Soc. **141**, 290-297 (2019)

8. Sumida, T., Dubiley, S., Wilcox, B., Severinov, K., Tagami, S.: Structural Basis of Leader Peptide Recognition in Lasso Peptide Biosynthesis Pathway. ACS Chem. Biol. **14**, 1619-1627 (2019)

9. Rosengren, K.J., Clark, R.J., Daly, N.L., Goeransson, U., Jones, A., Craik, D.J.: Microcin J25 Has a Threaded Sidechain-to-Backbone Ring Structure and Not a Head-to-Tail Cyclized Backbone. J. Am. Chem. Soc. **125**, 12464-12474 (2003)

10. Li, Y., Ducasse, R., Zirah, S., Blond, A., Goulard, C., Lescop, E., Giraud, C., Hartke, A., Guittet, E., Pernodet, J.L., Rebuffat, S.: Characterization of Sviceucin from Streptomyces Provides Insight into Enzyme Exchangeability and Disulfide Bond Formation in Lasso Peptides. ACS Chem. Biol. **10**, 2641-2649 (2015)

11. Knappe, T.A., Linne, U., Xie, X., Marahiel, M.A.: The glucagon receptor antagonist BI-32169 constitutes a new class of lasso peptides. FEBS Lett. **584**, 785-789 (2010)

12. Frechet, D., Guitton, J.D., Herman, F., Faucher, D., Helynck, G., Monegier du Sorbier, B., Ridoux, J.P., James-Surcouf, E., Vuilhorgne, M.: Solution structure of RP 71955, a new 21 amino acid tricyclic peptide active against HIV-1 virus. Biochemistry. **33**, 42-50 (1994)

13. Detlefsen, D.J., Hill, S.E., Volk, K.J., Klohr, S.E., Tsunakawa, M., Furumai, T., Lin, P.F., Nishio, M., Kawano, K., Oki, T., Lee, M.S.: Siamycins I and II, New Anti-HIV-1 Peptides: II. Sequence Analysis and Structure Determination of Siamycin I. J. Antibiot. **48**, 1515-1517 (1995)

14. Tietz, J.I., Schwalen, C.J., Patel, P.S., Maxson, T., Blair, P.M., Tai, H.C., Zakai, U.I., Mitchell, D.A.: A new genome-mining tool redefines the lasso peptide biosynthetic landscape. Nat. Chem. Biol. **13**, 470-478 (2017)

15. Hegemann, J.D., De Simone, M., Zimmermann, M., Knappe, T.A., Xie, X., Di Leva, F.S., Marinelli, L., Novellino, E., Zahler, S., Kessler, H., Marahiel, M.A.: Rational improvement of the affinity and selectivity of integrin binding of grafted lasso peptides. J. Med. Chem. **57**, 5829-5834 (2014)

16. Hegemann, J.D., Zimmermann, M., Zhu, S., Klug, D., Marahiel, M.A.: Lasso peptides from proteobacteria: Genome mining employing heterologous expression and mass spectrometry. Biopolymers. **100**, 527-542 (2013)

17. Zimmermann, M., Hegemann, J.D., Xie, X., Marahiel, M.A.: The astexin-1 lasso peptides: biosynthesis, stability, and structural studies. Chem. Biol. **20**, 558-569 (2013)

18. Hegemann, J.D., Fage, C.D., Zhu, S., Harms, K., Di Leva, F.S., Novellino, E., Marinelli, L., Marahiel, M.A.: The ring residue proline 8 is crucial for the thermal stability of the lasso peptide caulosegnin II. Mol. Biosyst. **12**, 1106-1109 (2016)

19. Knappe, T.A., Linne, U., Robbel, L., Marahiel, M.A.: Insights into the biosynthesis and stability of the lasso peptide capistruin. Chem. Biol. **16**, 1290-1298 (2009)

20. Hegemann, J.D.: Factors Governing the Thermal Stability of Lasso Peptides. ChemBioChem. **21**, 7-18 (2020)

21. Fage, C.D., Hegemann, J.D., Nebel, A.J., Steinbach, R.M., Zhu, S., Linne, U., Harms, K., Bange, G., Marahiel, M.A.: Structure and Mechanism of the Sphingopyxin I Lasso Peptide Isopeptidase. Angew. Chem. Int. Ed. Engl. **128**, 12909-12913 (2016)

22. Maksimov, M.O., Link, A.J.: Discovery and characterization of an isopeptidase that linearizes lasso peptides. J. Am. Chem. Soc. **135**, 12038-12047 (2013)

23. Xie, X., Marahiel, M.A.: NMR as an Effective Tool for the Structure Determination of Lasso Peptides. ChemBioChem. **13**, 621-625 (2012)

24. Hegemann, J.D., Jeanne Dit Fouque, K., Xie, X.: X Lasso Peptides: Structure, Biosynthesis, Activities, and Beyond. In: Elsevier (ed.). San Diego, (2020)

25. Nar, H., Schmid, A., Puder, C., Potterat, O.: High-resolution crystal structure of a lasso Peptide. ChemMedChem. **5**, 1689-1692 (2010)

26. Hegemann, J.D., Zimmermann, M., Zhu, S., Steuber, H., Harms, K., Xie, X., Marahiel, M.A.: Xanthomonins I-III: a new class of lasso peptides with a seven-residue macrolactam ring. Angew. Chem. Int. Ed. Engl. **53**, 2230-2234 (2014)

27. Jeanne Dit Fouque, K., Lavanant, H., Zirah, S., Hegemann, J.D., Fage, C.D., Marahiel, M.A., Rebuffat, S., Afonso, C.: General rules of fragmentation evidencing lasso structures in CID and ETD. Analyst. **143**, 1157-1170 (2018)

28. Perot-Taillandier, M., Zirah, S., Rebuffat, S., Linne, U., Marahiel, M.A., Cole, R.B., Tabet, J.C., Afonso, C.: Determination of peptide topology through time-resolved double-resonance under electron capture dissociation conditions. Anal. Chem. **84**, 4957-4964 (2012)

29. Jeanne Dit Fouque, K., Bisram, V., Hegemann, J.D., Zirah, S., Rebuffat, S., Fernandez-Lima, F.: Structural signatures of the class III lasso peptide BI-32169 and the branched-cyclic topoisomers using trapped ion mobility spectrometry-mass spectrometry and tandem mass spectrometry. Anal. Bioanal. Chem. **411**, 6287-6296 (2019)

30. Jeanne Dit Fouque, K., Moreno, J., Hegemann, J.D., Zirah, S., Rebuffat, S., Fernandez-Lima, F.: Identification of Lasso Peptide Topologies Using Native Nanoelectrospray Ionization-Trapped Ion Mobility Spectrometry-Mass Spectrometry. Anal. Chem. **90**, 5139-5146 (2018)

31. Jeanne Dit Fouque, K., Afonso, C., Zirah, S., Hegemann, J.D., Zimmermann, M., Marahiel, M.A., Rebuffat, S., Lavanant, H.: Ion mobility-mass spectrometry of lasso peptides: signature of a rotaxane topology. Anal. Chem. **87**, 1166-1172 (2015)

32. Zhu, S., Hegemann, J.D., Fage, C.D., Zimmermann, M., Xie, X., Linne, U., Marahiel, M.A.: Insights into the Unique Phosphorylation of the Lasso Peptide Paeninodin. J. Biol. Chem. **291**, 13662-13678 (2016)

33. Martin-Gomez, H., Linne, U., Albericio, F., Tulla-Puche, J., Hegemann, J.D.: Investigation of the Biosynthesis of the Lasso Peptide Chaxapeptin Using an E. coli-Based Production System. J. Nat. Prod. **81**, 2050-2056 (2018)

34. Jeanne Dit Fouque, K., Lavanant, H., Zirah, S., Steinmetz, V., Rebuffat, S., Maitre, P., Afonso, C.: IRMPD Spectroscopy: Evidence of Hydrogen Bonding in the Gas Phase Conformations of Lasso Peptides and their Branched-Cyclic Topoisomers. J. Phys. Chem. A. **120**, 3810-3816 (2016)

35. Fernandez-Lima, F.A., Kaplan, D.A., Park, M.A.: Note: Integration of trapped ion mobility spectrometry with mass spectrometry. Rev. Sci. Instrum. **82**, 126106 (2011)

36. Fernandez-Lima, F.A., Kaplan, D.A., Suetering, J., Park, M.A.: Gas-phase separation using a Trapped Ion Mobility Spectrometer. Int. J. Ion Mobil. Spectrom. **14**, 93-98 (2011)

37. Hernandez, D.R., Debord, J.D., Ridgeway, M.E., Kaplan, D.A., Park, M.A., Fernandez-Lima, F.: Ion dynamics in a trapped ion mobility spectrometer. Analyst. **139**, 1913-1921 (2014)

38. Ridgeway, M.E., Lubeck, M., Jordens, J., Mann, M., Park, M.A.: Trapped ion mobility spectrometry: A short review. Int. J. Mass Spectrom. **425**, 22-35 (2018)

39. Bakker, J.M., Besson, T., Lemaire, J., Scuderi, D., Maitre, P.: Gas-phase structure of a pi-allyl-palladium complex: efficient infrared spectroscopy in a 7 T Fourier transform mass spectrometer. J. Phys. Chem. A. **111**, 13415-13424 (2007)

40. Prazeres, R., Glotin, F., Insa, C., Jaroszynski, D.A., Ortega, J.M.: Two-colour operation of a Free-Electron Laser and applications in the mid-infrared. Eur. Phys. J. D. **3**, 87-93 (1998)

41. Svendsen, A., Lorenz, U.J., Boyarkin, O.V., Rizzo, T.R.: A new tandem mass spectrometer for photofragment spectroscopy of cold, gas-phase molecular ions. Rev. Sci. Instrum. **81**, 073107 (2010)

42. Zabuga, A.V., Kamrath, M.Z., Boyarkin, O.V., Rizzo, T.R.: Fragmentation mechanism of UV-excited peptides in the gas phase. J. Chem. Phys. **141**, 154309 (2014)

43. Scutelnic, V., Perez, M.A.S., Marianski, M., Warnke, S., Gregor, A., Rothlisberger, U., Bowers, M.T., Baldauf, C., von Helden, G., Rizzo, T.R., Seo, J.: The Structure of the Protonated Serine Octamer. J. Am. Chem. Soc. **140**, 7554-7560 (2018)

44. Zirah, S., Afonso, C., Linne, U., Knappe, T.A., Marahiel, M.A., Rebuffat, S., Tabet, J.-C.: Topoisomer Differentiation of Molecular Knots by FTICR MS: Lessons from Class II Lasso Peptides. J. Am. Soc. Mass Spectrom. **22**, 467-479 (2011)

45. Jeanne Dit Fouque, K., Lavanant, H., Zirah, S., Hegemann, J.D., Zimmermann, M., Marahiel, M.A., Rebuffat, S., Afonso, C.: Signatures of Mechanically Interlocked Topology of Lasso Peptides by Ion Mobility-Mass Spectrometry: Lessons from a Collection of Representatives. J. Am. Soc. Mass Spectrom. **28**, 315-322 (2017)

46. Jeanne Dit Fouque, K., Lavanant, H., Zirah, S., Lemoine, J., Rebuffat, S., Tabet, J.C., Kulesza, A., Afonso, C., Dugourd, P., Chirot, F.: Gas-phase conformations of capistruin - comparison of lasso, branched-cyclic and linear topologies. Rapid Commun. Mass Spectrom. **29**, 1411-1419 (2015)

47. Hernandez, O., Isenberg, S., Steinmetz, V., Glish, G.L., Maitre, P.: Probing Mobility-Selected Saccharide Isomers: Selective Ion-Molecule Reactions and Wavelength-Specific IR Activation. J. Phys. Chem. A. **119**, 6057-6064 (2015)

48. Patrick, A.L., Stedwell, C.N., Polfer, N.C.: Differentiating sulfopeptide and phosphopeptide ions via resonant infrared photodissociation. Anal. Chem. **86**, 5547-5552 (2014)

49. Stedwell, C.N., Patrick, A.L., Gulyuz, K., Polfer, N.C.: Screening for phosphorylated and nonphosphorylated peptides by infrared photodissociation spectroscopy. Anal. Chem. **84**, 9907-9912 (2012)

50. Wassermann, T.N., Boyarkin, O.V., Paizs, B., Rizzo, T.R.: Conformation-specific spectroscopy of peptide fragment ions in a low-temperature ion trap. J. Am. Soc. Mass Spectrom. **23**, 1029-1045 (2012)

51. Giubertoni, G., Sofronov, O.O., Bakker, H.J.: Effect of intramolecular hydrogen-bond formation on the molecular conformation of amino acids. Commun. Chem. **3**, (2020)

52. Plowright, R.J., Gloaguen, E., Mons, M.: Compact folding of isolated four-residue neutral peptide chains: H-bonding patterns and entropy effects. ChemPhysChem. **12**, 1889-1899 (2011)

53. Scuderi, D., Bakker, J.M., Durand, S., Maitre, P., Sharma, A., Martens, J.K., Nicol, E., Clavaguéra, C., Ohanessian, G.: Structure of singly hydrated, protonated phospho-tyrosine. Int. J. Mass Spectrom. **308**, 338-347 (2011)

54. Kusaka, R., Zhang, D., Walsh, P.S., Gord, J.R., Fisher, B.F., Gellman, S.H., Zwier, T.S.: Role of ring-constrained gamma-amino acid residues in alpha/gamma-peptide folding: single-conformation UV and IR spectroscopy. J. Phys. Chem. A. **117**, 10847-10862 (2013)

55. Burke, N.L., Redwine, J.G., Dean, J.C., McLuckey, S.A., Zwier, T.S.: UV and IR spectroscopy of cold protonated leucine enkephalin. Int. J. Mass Spectrom. **378**, 196-205 (2015)

56. Rijs, A.M., Kabelac, M., Abo-Riziq, A., Hobza, P., de Vries, M.S.: Isolated gramicidin peptides probed by IR spectroscopy. ChemPhysChem. **12**, 1816-1821 (2011)

57. Kupser, P., Pagel, K., Oomens, J., Polfer, N., Koksch, B., Meijer, G., von Helden, G.: Amide-I and -II vibrations of the cyclic beta-sheet model peptide gramicidin S in the gas phase. J. Am. Chem. Soc. **132**, 2085-2093 (2010)

58. Stedwell, C.N., Galindo, J.F., Gulyuz, K., Roitberg, A.E., Polfer, N.C.: Crown complexation of protonated amino acids: influence on IRMPD spectra. J. Phys. Chem. A. **117**, 1181-1188 (2013)

59. Lucas, B., Lecomte, F., Reimann, B., Barth, H.-D., Grégoire, G., Bouteiller, Y., Schermann, J.-P., Desfrançois, C.: A new infrared spectroscopy technique for structural studies of mass-selected neutral polar complexes without chromophore. Phys. Chem. Chem. Phys. **6**, 2600 (2004)

60. Stearns, J.A., Mercier, S., Seaiby, C., Guidi, M., Boyarkin, O.V., Rizzo, T.R.: Conformation-specific spectroscopy

and photodissociation of cold, protonated tyrosine and phenylalanine. J. Am. Chem. Soc. **129**, 11814-11820 (2007)

61. Kopysov, V., Boyarkin, O.V.: Resonance Energy Transfer Relates the Gas-Phase Structure and Pharmacological Activity of Opioid Peptides. Angew. Chem. Int. Ed. Engl. **55**, 689-692 (2016)

62. Ducasse, R., Yan, K.P., Goulard, C., Blond, A., Li, Y., Lescop, E., Guittet, E., Rebuffat, S., Zirah, S.: Sequence determinants governing the topology and biological activity of a lasso peptide, microcin J25. ChemBioChem. **13**, 371-380 (2012)

For Table of Contents Only